

Lateral β-Ga_2O_3 Schottky barrier diode fabricated on (-201) single crystal substrate and its temperature-dependent current-voltage characteristics

Pei-Pei Ma(马培培), Jun Zheng(郑军), Ya-Bao Zhang(张亚宝), Xiang-Quan Liu(刘香全), Zhi Liu(刘智), Yu-Hua Zuo(左玉华), Chun-Lai Xue(薛春来), and Bu-Wen Cheng(成步文)

Citation: Chin. Phys. B, 2022, 31 (**4**): 047302. DOI: 10.1088/1674-1056/ac2729

Journal homepage: http://cpb.iphy.ac.cn; http://iopscience.iop.org/cpb

What follows is a list of articles you may be interested in

Lateral β-Ga_2O_3 Schottky barrier diode fabricated on (-201) single crystal substrate and its temperature-dependent current-voltage characteristics

Pei-Pei Ma(马培培), Jun Zheng(郑军), Ya-Bao Zhang(张亚宝), Xiang-Quan Liu(刘香全), Zhi Liu(刘智), Yu-Hua Zuo(左玉华), Chun-Lai Xue(薛春来), and Bu-Wen Cheng(成步文)

Chin. Phys. B, 2022, 31 (**4**): 047302. DOI: 10.1088/1674-1056/ac2729

Design and simulation of AlN-based vertical Schottky barrier diodes

Chun-Xu Su(苏春旭), Wei Wen(温暐), Wu-Xiong Fei(费武雄), Wei Mao(毛维), Jia-Jie Chen(陈佳杰), Wei-Hang Zhang(张苇杭), Sheng-Lei Zhao(赵胜雷), Jin-Cheng Zhang(张进成), and Yue Hao(郝跃)

Chin. Phys. B, 2021, 30 (**6**): 067305. DOI: 10.1088/1674-1056/abe0c7

Device topological thermal management of β-Ga_2O_3 Schottky barrier diodes

Yang-Tong Yu(俞扬同), Xue-Qiang Xiang(向学强), Xuan-Ze Zhou(周选择), Kai Zhou(周凯), Guang-Wei Xu(徐光伟), Xiao-Long Zhao(赵晓龙), and Shi-Bing Long(龙世兵)

Chin. Phys. B, 2021, 30 (**6**): 067302. DOI: 10.1088/1674-1056/abeee2

High-responsivity solar-blind photodetector based on MOCVD-grown Si-doped β-Ga_2O_3 thin film

Yu-Song Zhi(支钰崧), Wei-Yu Jiang(江为宇), Zeng Liu(刘增), Yuan-Yuan Liu(刘媛媛), Xu-Long Chu(褚旭龙), Jia-Hang Liu(刘佳航), Shan Li(李山), Zu-Yong Yan(晏祖勇), Yue-Hui Wang(王月晖), Pei-Gang Li(李培刚), Zhen-Ping Wu(吴真平), and Wei-Hua Tang(唐为华)

Chin. Phys. B, 2021, 30 (**5**): 057301. DOI: 10.1088/1674-1056/abe37a

Self-powered solar-blind photodiodes based on EFG-grown (100)-dominant β-Ga_2O_3 substrate

Xu-Long Chu(褚旭龙), Zeng Liu(刘增), Yu-Song Zhi(支钰崧), Yuan-Yuan Liu(刘媛媛), Shao-Hui Zhang(张少辉), Chao Wu(吴超), Ang Gao(高昂), Pei-Gang Li(李培刚), Dao-You Guo(郭道友), Zhen-Ping Wu(吴真平), and Wei-Hua Tang(唐为华)

Chin. Phys. B, 2021, 30 (**1**): 017302. DOI: 10.1088/1674-1056/abc546

Lateral β-Ga_2O_3 Schottky barrier diode fabricated on (–201) single crystal substrate and its temperature-dependent current–voltage characteristics

Pei-Pei Ma(马培培)[1,2], Jun Zheng(郑军)[1,2,†], Ya-Bao Zhang(张亚宝)[1,2], Xiang-Quan Liu(刘香全)[1,2], Zhi Liu(刘智)[1,2], Yu-Hua Zuo(左玉华)[1,2], Chun-Lai Xue(薛春来)[1,2], and Bu-Wen Cheng(成步文)[1,2]

[1] *State Key Laboratory on Integrated Optoelectronics, Institute of Semiconductors, Chinese Academy of Sciences, Beijing* 100083, *China*
[2] *Center of Materials Science and Optoelectronics Engineering, University of Chinese Academy of Sciences, Beijing* 100049, *China*

(Received 2 July 2021; revised manuscript received 8 September 2021; accepted manuscript online 16 September 2021)

Lateral β-Ga_2O_3 Schottky barrier diodes (SBDs) each are fabricated on an unintentionally doped (-201) n-type β-Ga_2O_3 single crystal substrate by designing L-shaped electrodes. By introducing sidewall electrodes on both sides of the conductive channel, the SBD demonstrates a high current density of 223 mA/mm and low specific on-resistance of 4.7 mΩ·cm^2. Temperature-dependent performance is studied and the Schottky barrier height is extracted to be in a range between 1.3 eV and 1.35 eV at temperatures ranging from 20 °C to 150 °C. These results suggest that the lateral β-Ga_2O_3 SBD has a tremendous potential for future power electronic applications.

Keywords: β-Ga_2O_3, Schottky barrier diodes, rectifying ability, breakdown voltage

PACS: 73.40.Mr, 84.30.Jc, 85.30.De, 85.30.Kk **DOI:** 10.1088/1674-1056/ac2729

1. Introduction

Recently, gallium oxide (Ga_2O_3) has received much attention because of its unique properties,[1–3] including a wide bandgap (4.5 eV–4.8 eV) and a high breakdown electric field of 8 MV/cm. The Baliga's figure of merit of β-Ga_2O_3 reaches up to 3444, which is significantly higher than that of silicon carbide (SiC) and gallium nitride (GaN).[4–6] Moreover, high-quality large-size single-crystal β-Ga_2O_3 substrates can be easily grown by low-cost and stable melting methods.[7–10] Thus, β-Ga_2O_3 materials have great potential applications in power devices. In power electronic circuits, two types of power devices each play a key role in power conversion. The first type is the switching transistor, which controls the switching state of the current transmission to regulate the total power, and the second type is the rectifier diode, which controls the transmission direction of the current. As the P-type doping technology of β-Ga_2O_3 materials is very difficult, β-Ga_2O_3 wafers are all of n-type semiconductor and more applicable for unipolar power devices, such as metal–oxide–semiconductor field-effect transistors (MOSFETs) and Schottky barrier diodes (SBDs).[11,12] Considerable efforts have been made to enhance the performances of β-Ga_2O_3 power devices, and remarkable results have been achieved. For example, field-plated MOSFETs each with a high breakdown voltage (BV)[13] and high power figure of merit (P-FOM)[14] have been reported.

The SBDs are important for power rectification applications due to their advantages of low turn-on voltage, fast switching speed, and low switching loss.[15,16] The β-Ga_2O_3 SBDs reported possess almost vertical structures by homoepitaxy of high-quality β-Ga_2O_3 drift layers.[17–21] For example, Allen *et al.* reported that vertical structured SBD with a breakdown electric field of up to 3.5 MV/cm involves an edge termination and a small-angle beveled field plate.[22] Li *et al.* reported vertical trench SBD with a BV of 2.89 kV and PFOM of 0.95 GW/cm^2.[23] Unlike vertical SBD structure, the lateral SBD structure can be fabricated on single-crystal β-Ga_2O_3 substrate with the highest quality drift layer, while avoiding the difficult and costly hydride vapor phase epitaxy homoepitaxial growth techniques. However, the current flowing in a lateral structure device is limited in the extremely thin channel layer; therefore, there are few reports on lateral β-Ga_2O_3 SBDs.[24–26] For example, lateral SBD with the highest forward current density of 40 mA/mm has been fabricated by transferring β-Ga_2O_3 nano-membranes.

In this study, we fabricate lateral SBDs on high-quality single-crystal β-Ga_2O_3 substrates by designing L-shaped electrodes. By introducing the sidewall electrodes on both sides of the conductive channel, the high forward current density of 223 mA/mm and the low specific on resistance ($R_{on,sp}$) of 4.7 mΩ·cm^2 are achieved. In addition, the device shows a high reverse voltage and good rectifying ability. These results indicate that lateral β-Ga_2O_3 SBDs have great potential applications in power electronics.

†Corresponding author. E-mail: zhengjun@semi.ac.cn

© 2022 Chinese Physical Society and IOP Publishing Ltd

2. Experimental details

The unintentionally doped (UID) (-201) n-type β-Ga_2O_3 bulk crystal with carrier concentration about was 2.2×10^{17} cm^{-3} used in this work for fabricating lateral SBD. Figure 1(a) shows the high resolution x-ray diffraction (HRXRD) 2θ–ω scans of the β-Ga_2O_3 substrate to characterize the crystal quality. A schematic of the device is shown in Fig. 1(b). The conductive channels of carriers were designed along the [010] direction, which has high carrier mobility. Moreover, it was found that the dry etch has low damage to the (010) sidewalls, providing the high performance of lateral SBD. The lateral β-Ga_2O_3 SBD structure was fabricated by depositing a 300-nm-thick passivation layer on the top of the substrate by plasma-enhanced chemical vapor deposition (PECVD). The cathode and anode regions were shaped by dry etching,[27] respectively. The Si implantation and annealing treatment were performed in the cathode region of the sidewall and bottom mesa to form an ohmic contact.[28] The doping concentration is estimated at $\sim 5\times10^{19}$ cm^{-3}, based on the simulation. After Si activation, the Ti/Au electrodes were evaporated and implemented rapid thermal annealing (RTA) at 475 °C for 1 min. Based on the transfer length method (TLM), the sheet resistance (R_{SH}) and contact resistance (R_C) were extracted to be 176 Ω and 1 Ω·mm, respectively. Finally, a Schottky contact was introduced by stacking metals of Ni/Au, followed by the steps of device passivation, pads opening and metal thickening. An optical micrograph of the fabricated device is shown in Fig. 1(c). The current–voltage characterizations were tested in the dark by using an Agilent B1500A semiconductor parameter analyzer. The reverse breakdown characterizations were performed by using a Keithley 4200-SCS.

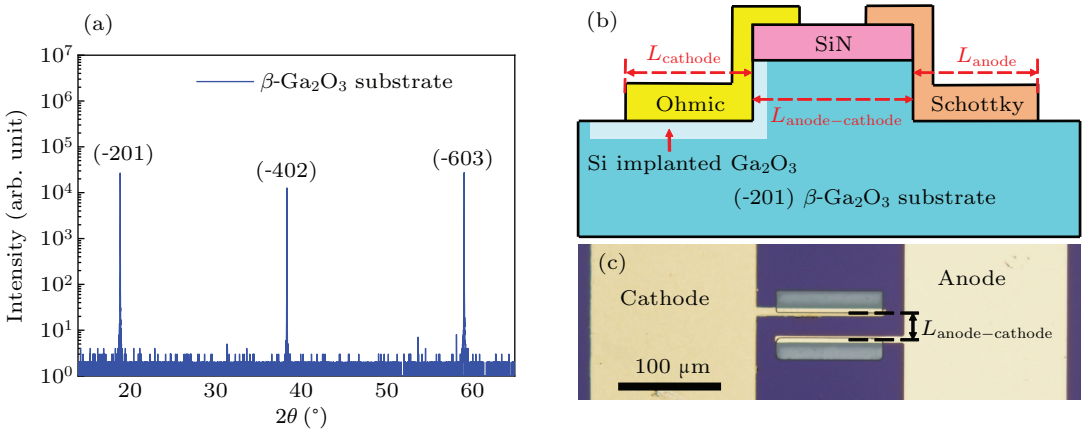


Fig. 1. (a) HRXRD curve of (-201) β-Ga_2O_3 single crystal substrate, (b) schematic diagram of device cross-section, and (c) optical micrograph of a fabricated SBD.

3. Results and discussion

Figure 2(a) shows the forward J–V on a linear scale and differential resistance–voltage (Diff. R_{on}–V) characteristics for lateral SBDs with different values of L_{AC}. From the DC measurements, a current density of 223 mA/mm, which is one order of magnitude higher than the current density of the reported lateral β-Ga_2O_3 SBDs,[24,25] and a very low V_{on} is achieved to be 0.98 V. The anode length (L_A) and the cathode length (L_C) are 5 μm. The value of Diff. R_{on} is extracted to be 13.5 Ω·mm, yielding the value of $R_{on,sp}$ of 4.7 mΩ·cm^2 for $L_{AC} = 25$ μm by considering that $R_{on,sp} = R_{on} \times (L_A + L_{AC} + L_C)$. Figure 2(b) shows the forward current density–voltage (J–V) characteristics of the lateral SBD with $L_{AC} = 25$ μm on a semi-logarithmic scale. The I_{on}/I_{off} ratio is as high as 10^9. A subthreshold swing of 67 mV/dec is extracted from the current density between 10^{-6} mA/mm and 10^{-3} mA/mm. Figure 2(c) demonstrates that the measured current is nearly proportional to the device width.

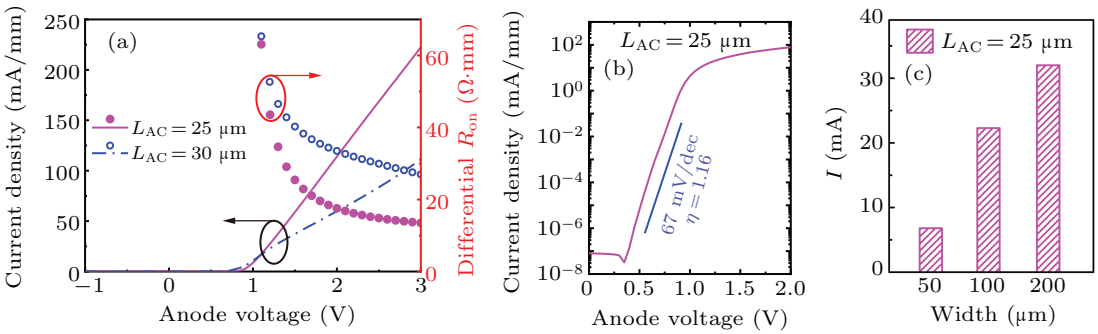


Fig. 2. (a) Linear-scale plots of forward J–V and Diff. R_{on}–V characteristics, (b) log-scale forward J–V characteristics of the fabricated lateral SBD with $L_{AC} = 25$ μm, and (c) dependence of current on the width of SBD for $L_{AC} = 25$ μm.

Figure 3 shows the reverse I–V characteristic of the β-Ga_2O_3 SBD. The device can withstand a reverse voltage as high as 200 V without breakdown, much higher than other β-Ga_2O_3 SBDs using single crystals[29] and lateral GaN SBDs.[15] We cannot further increase the voltage for testing due to the limitation of the test instrument. Moreover, the breakdown voltage will be larger than 200 V, for the reverse current value is about 10^{-7} A under the maximum test voltage.

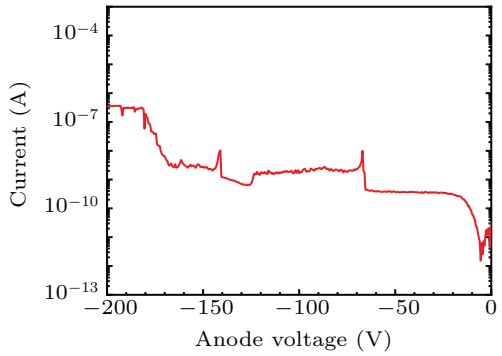


Fig. 3. Reverse I–V characteristic of Ni/β-Ga_2O_3 SBD with $L_{AC} = 30$ μm.

According to the thermionic emission (TE) model, the forward J–V relationship can be expressed by the equation of

$$J = J_0 \exp\left(\frac{qV}{\eta kT}\right)\left[1 - \exp\left(-\frac{qV}{kT}\right)\right],$$

where J_0 represents the saturation current density which can be expressed as

$$J_0 = A^* T^2 \exp\left(-\frac{q\Phi_{b,0}}{kT}\right),$$

and η is the ideality factor, where the effective Richardson's constant

$$A^* = \frac{4\pi q m^* k^2}{h^3} = 1.201 \times 10^2 \left(\frac{m^*}{m_0}\right) [\mathrm{A/cm^2 \cdot K^2}]$$
$$= 27.623 \sim 40.834\ \mathrm{A/cm^2 \cdot K^2}$$

using $m^* = 0.23m_0 \sim 0.34m_0$ calculated from first-principles;[17,30] $q\Phi_{b,0}$ is the height of Schottky barrier at zero bias and given by $q\Phi_{b,0} = qV_{bi} + (E_c - E_f) - q\Phi_{ifbl}$, with qV_{bi}, E_c, E_f, and $q\Delta\Phi_{ifbl}$ being the zero bias built-in potential, minimum value of conduction band, Fermi level, and potential barrier reduction caused by image force.

The forward temperature-dependent J–V characteristics of the β-Ga_2O_3 SBD in a semi-logarithmic scale are measured as shown in Fig. 4(a). By increasing the working temperature from 20 °C to 150 °C in steps of 25 °C, these characteristics evolve smoothly. Analysis of the linear region of the log$J$–V plot shows that J_0 and η can be calculated from the slope and intercept. Figure 4(b) is Richardson's plot, that is, the $[\ln(J_0/T^2) - 1/kT]$ plot. By fitting the test data linearly, $q\Phi_{b,0}$ and A^* are obtained from slope and intercept, respectively, to be $q\Phi_{b,0} = 1.3$ eV and $A^* = 29.7$ A/cm^2·K^2. The extracted $q\Phi_{b,0}$ values is higher than those of Ni/Ga_2O_3[19,20,24] and TiN/Ga_2O_3 Schottky contact,[26] and even higher than that of Pt/Ga_2O_3 contact.[17] The high $q\Phi_{b,0}$ is mainly caused by the low doping concentration of the UID wafer.[23,31] Moreover, the A^* value is smaller than other reported experimental results[17,18] but matches well with previous first-principles calculation results. The lower A^* may be due to the low effective density of states in the conduction band[32] or the uneven distribution of Schottky barrier.[33] Figure 4(c) also displays the plots of the temperature dependence of $q\Phi_{b,0}$ and η derived by fitting the J–V curves, showing they slightly decrease to about 1.30 ± 0.05 eV and 1.16 ± 0.05 eV as the temperature increases from 20 °C to 150 °C. Both the $q\Phi_{b,0}$ values obtained from the Richardson's plot and fitted J–V curves are in accordance with each other. The reason for a weak temperature dependence of $q\Phi_{b,0}$ is that E_c–E_f has a positive temperature coefficient while qV_{bi} is negatively correlated with temperature. As the temperature increases, more electrons have enough energy to cross the barrier, resulting in slight decrease of $q\Phi_{b,0}$ and η.[17]

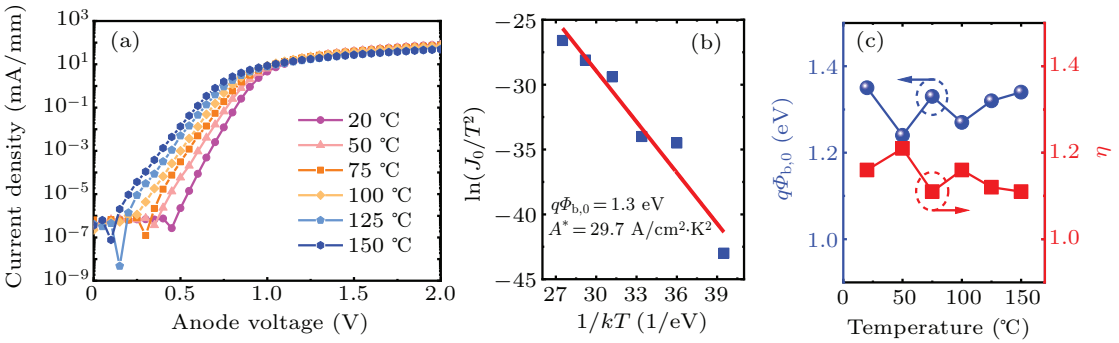


Fig. 4. (a) Forward J–V–T characteristics on a log scale of lateral SBD with $L_{AC} = 25$ μm in a temperature range of 20 °C–150 °C, (b) Richardson's plot of lateral SBD with $L_{AC} = 25$ μm, and (c) temperature dependence of extracted $q\Phi_{b,0}$ and η.

The benchmark performances of some state-of-the-art representative β-Ga_2O_3 SBDs with marked vertical and lateral structures, are shown in Table 1. It is evident that the SBD in this work shows the highest forward current density among all the lateral β-Ga_2O_3 SBDs reported so far. Moreover, in this work, the SBD presents an extremely low $R_{on,sp}$ because it is fabricated on

a high-quality single substrate with low dislocation.[34] By thickening the β-Ga_2O_3 etching depth to enlarge the metal contact profile, the forward current density can be further enhanced as the $R_{on,sp}$ will be reduced,[16] whereas the $R_{on,sp}$ of vertical SBD can only be reduced by increasing the carrier concentration at the cost of reduced BV.

Table 1. Comparison among characteristic parameters of β-Ga_2O_3 SBDs.

SBDs	Current density	$R_{on,sp}$ (mΩ·cm^2)	Ref.
β-Ga_2O_3 drift layers	10 A/cm^2	25	[19]
β-Ga_2O_3 single crystal	56 A/cm^2	12.5	[18]
β-Ga_2O_3 trench	150 A/cm^2	10.5	[23]
β-Ga_2O_3 nano-membranes	30 mA/mm	10.2	[24]
β-Ga_2O_3 nano-membranes	40 mA/mm	–	[25]
$\beta-Ga_2O_3$ single crystal	223 mA/mm	4.7	this work

4. Conclusions

In this work, the lateral β-Ga_2O_3 SBDs each with an innovative structure adopting an unintentionally doped (-201) β-Ga_2O_3 single crystal have been demonstrated. The fabricated devices each with a simple L-shaped electrode structure exhibit outstanding forward current density and low $R_{on,sp}$ with respect to other lateral SBDs. The lateral SBD fabricated on β-Ga_2O_3 single crystal substrate has a high-quality drift channel in comparison with those fabricated by homoepitaxial techniques. The lateral SBDs in this work have broad applications, and may serve as an promising candidate for future high-power electronic devices.

Acknowledgements

Project supported by the National Key Research and Development Program of China (Grant No. 2018YFB2200500), the National Natural Science Foundation of China (Grant Nos. 62050073, 62090054, and 61975196), and the Key Research Program of Frontier Sciences, Chinese Academy of Sciences (Grant No. QYZDY-SSW-JSC022).

References

[1] Millan J, Godignon P, Perpina X, Perez-Tomas A and Rebollo J 2014 *IEEE Trans. Power Electron.* **29** 2155
[2] Qin Y, Long S B, Dong H, He Q M, Jian G Z, Zhang Y, Hou X H, Tan P J, Zhang Z F, Lv H B, Liu Q and Liu M 2019 *Chin. Phys. B* **28** 018501
[3] Liu Z, Li P G, Zhi Y S, Wang X L, Chu X L and Tang W H 2019 *Chin. Phys. B* **28** 017105
[4] Pearton S J, Yang J C, Cary P H, Ren F, Kim J, Tadjer M J and Mastro M A 2018 *Appl. Phys. Rev.* **5** 011301
[5] Zhang H P, Yuan L, Tang X Y, Hu J C, Sun J W, Zhang Y M, Zhang Y M and Jia R X 2020 *IEEE Trans. Power Electron.* **35** 5157
[6] Dong H, Xue H W, He Q M, Qin Y, Jian G Z, Long S B and Liu M 2019 *J. Semicond.* **40** 011802
[7] Galazka Z, Irmscher K, Schewski R, Hanke I M, Pietsch M, Ganschow S, Klimm D, Dittmar A, Fiedler A, Schroeder T and Bickermann M 2020 *J. Cryst. Growth* **529** 125297
[8] Galazka Z, Irmscher K, Uecker R, Bertram R, Pietsch M, Kwasniewski A, Naumann M, Schulz T, Schewski R, Klimm D and Bickermann M 2014 *J. Cryst. Growth* **404** 184
[9] Mu W X, Jia Z T, Yin Y R, Hu Q Q, Li Y, Wu B Y, Zhang J and Tao X T 2017 *J. Alloys Compd.* **714** 453
[10] Mohamed H F, Xia C T, Sai Q L, Cui H Y, Pan M Y and Qi H J 2019 *J. Semicond.* **40** 011801
[11] Xu Y, Chen X H, Cheng L, Ren F F, Zhou J J, Bai S, Lu H, Gu S L, Zhang R, Zheng Y D and Ye J D 2019 *Chin. Phys. B* **28** 038503
[12] Wang H, Jiang L L, Lin X P, Lei S Q and Yu H Y 2018 *Chin. Phys. B* **27** 127302
[13] Sharma S, Zeng K, Saha S and Singisetti U 2020 *IEEE Electron Dev. Lett.* **41** 836
[14] Lv Y J, Liu H Y, Zhou X Y, Wang Y G, Song X B, Cai Y C, Yan Q L, Wang C L, Liang S X, Zhang J C, Feng Z H, Zhou H, Cai S J and Hao Y 2020 *IEEE Electron Dev. Lett.* **41** 537
[15] Dang K, Zhang J C, Zhou H, Huang S, Zhang T, Bian Z K, Zhang Y C, Wang X H, Zhao S L, Wei K and Hao Y 2020 *IEEE Trans. Power Electron.* **35** 2247
[16] Lu Y, Zhou F, Xu W, Wang D, Xia Y, Zhu Y, Pan D, Ren F, Zhou D, Ye J, Chen D, Zhang R, Zheng Y and Lu H 2020 *Appl. Phys. Express* **13** 096502
[17] Higashiwaki M, Konishi K, Sasaki K, Goto K, Nomura K, Thieu Q T, Togashi R, Murakami H, Kumagai Y, Monemar B, Koukitu A, Kuramata A and Yamakoshi S 2016 *Appl. Phys. Lett.* **108** 133503
[18] He Q M, Mu W X, Dong H, Long S B, Jia Z T, Lv H B, Liu Q, Tang M H, Tao X T and Liu M 2017 *Appl. Phys. Lett.* **110** 093503
[19] Yang J C, Ahn S, Ren F, Pearton S J, Jang S and Kuramata A 2017 *IEEE Electron Dev. Lett.* **38** 906
[20] Jayawardena A, Ahyi A C and Dhar S 2016 *Semicond. Sci. Technol.* **31** 115002
[21] Hu Z Z, Lv Y J, Zhao C Y, Feng Q, Feng Z Q, Dang K, Tian X S, Zhang Y C, Ning J, Zhou H, Kang X W, Zhang J C and Hao Y 2020 *IEEE Electron Dev. Lett.* **41** 441
[22] Allen N, Xiao M, Yan X D, Sasaki K, Tadjer M J, Ma J H, Zhang R Z, Wang H and Zhang Y H 2019 *IEEE Electron Dev. Lett.* **40** 1399
[23] Li W S, Nomoto K, Hu Z Y, Jena D and Xing H G 2020 *IEEE Electron Dev. Lett.* **41** 107
[24] Hu Z Z, Zhou H, Feng Q, Zhang J C, Zhang C F, Dang K, Cai Y C, Feng Z Q, Gao Y Y, Kang X W and Hao Y 2018 *IEEE Electron Dev. Lett.* **39** 1564
[25] Hu Z Z, Zhou H, Dang K, Cai Y C, Feng Z Q, Gao Y Y, Feng Q, Zhang J C and Hao Y 2018 *IEEE J. Electron Dev. Soc.* **6** 815
[26] Wang Y B, Xu W H, Han G Q, You T G, Mu F W, Hu H D, Liu Y, Zhang X C, Huang H, Suga T, Ou X, Ma X H and Hao Y 2020 *J. Phys. D: Appl. Phys.* **54** 034004
[27] Zhang L H, Verma A, Xing H L and Jena D 2017 *Jpn. J. Appl. Phys.* **56** 030304
[28] Ma P P, Zheng J, Zhang Y B, Liu Z, Zuo Y H and Cheng B W 2021 *Tsinghua Sci. Technol.*
[29] Sasaki K, Higashiwaki M, Kuramata A, Masui T and Yamakoshi S 2013 *IEEE Electron Dev. Lett.* **34** 493
[30] He H Y, Orlando R, Blanco M A, Pandey R, Amzallag E, Baraille I and Rérat M 2006 *Phys. Rev. B* **74** 195123
[31] Jian G Z, He Q M, Mu W X, Fu B, Dong H, Qin Y, Zhang Y, Xue H W, Long S B, Jia Z T, Lv H B, Liu Q, Tao X T and Liu M 2018 *AIP Adv.* **8** 015316
[32] Crowell C R 1965 *Solid State Electron.* **8** 395
[33] Long Z, Xia X C, Shi J J, Liu J, Geng X L, Zhang H Z and Liang H W 2020 *Acta Phys. Sin.* **69** 138501 (in Chinese)
[34] Fu B, Jia Z T, Mu W X, Yin Y R, Zhang J and Tao X T 2019 *J. Semicond.* **40** 011804